

Cyclic degradation of antagonistic shape memory actuated structures

A Y N Sofla, D M Elzey and H N G Wadley

Materials Science and Engineering Department, University of Virginia, Charlottesville, VA 22904, USA

E-mail: aarash@virginia.edu

Received 14 September 2007, in final form 7 January 2008

Published 11 February 2008

Online at stacks.iop.org/SMS/17/025014

Abstract

Antagonistic shape memory actuated structures exploit opposing pairs of one-way shape memory alloy (SMA) linear actuators to create devices capable of a fully reversible response. Unlike many conventional reversible SMA devices they do not require bias force components (springs) to return them to their pre-actuated configuration. However, the repeated use of SMA antagonistic devices results in the accumulation of plastic strain in the actuators which can diminish their actuation stroke. We have investigated this phenomenon and the effect of shape memory alloy pre-strain upon it for near equi-atomic NiTi actuators. We find that the degradation eventually stabilizes during cycling. A thermomechanical treatment has been found to significantly reduce degradation in cyclic response of the actuators.

(Some figures in this article are in colour only in the electronic version)

1. Introduction

Equi-atomic NiTi alloys undergo a martensitic transformation upon cooling below a critical temperature [1]. Significant inelastic straining of the martensite structure can occur by de-twinning of the martensite variants during subsequent deformation below the martensite start temperature, M_s . It can also be accompanied by dislocation nucleation and propagation [1]. A reverse martensite transformation occurs in these alloys upon heating above their austenite start temperature, A_s , which eliminates the de-twinning strain leading to the well known shape memory effect (SME) [1]. Large recovery forces are created in mechanically constrained shape memory alloy (SMA) samples upon heating above the A_s temperature. The combination of a relatively large recovered strain (several per cent) and high recovery stress (several hundred MPa) by NiTi SMAs has led to many applications for mechanical actuation [1]. Examples include their use in micro-electromechanical systems (MEMS) [2–4] and large-scale deployable structures [5]. The contractile response described above is often referred to as the one-way SME to distinguish it from a trained two-way effect that can be created by thermomechanical cycling of some alloys [1].

Reversible SMA actuated structures can be designed by placing pairs of linear SMA actuators (in the form of wire or ribbons) in an antagonistic arrangement. This antagonistic

or differential method [6] can be combined with a flexural structure such as a beam that can be bent or flexed in either direction about its neutral axis by actuation of one or other of the SMA actuators [7–11]. Figure 1 gives a simple example of such an actuated beam. It is composed of linearly repeated antagonistic flexural unit cells (AFC) [10]. Contraction (by heating) of either of the one-way actuators deforms the AFC while antagonistically extending the other one. Such a device therefore requires no spring system to enable its reuse.

A strain actuation capability is imparted to the AFC by mechanically stretching at least one of the two actuators in the cell at low temperature when the SMA is in either its martensitic or R-phase state [11] prior to assembly of the cell. This pre-strain in say actuator 1 is denoted ε_1^s while that in actuator 2 is ε_2^s (figure 1). Heating either of the pre-strained actuators in the AFC causes it to contract and to rotate the cell. This rotation requires extension of actuator 2 and a remnant strain, ε , in actuator 1. Given a prescribed pre-strain for actuator 1, the cell rotation angle, θ , depends only on the cell geometry and is given by [10]

$$\theta = 2 \tan^{-1}(L/H) - \cos^{-1} \left[1 - \frac{2(1 + \varepsilon - \varepsilon_1^s)^2}{1 + (H/L)^2} \right] \quad (1)$$

where L is the length of the SMA actuator in the initial configuration (prior to the activation of the assembled cell) and H is the cell height.

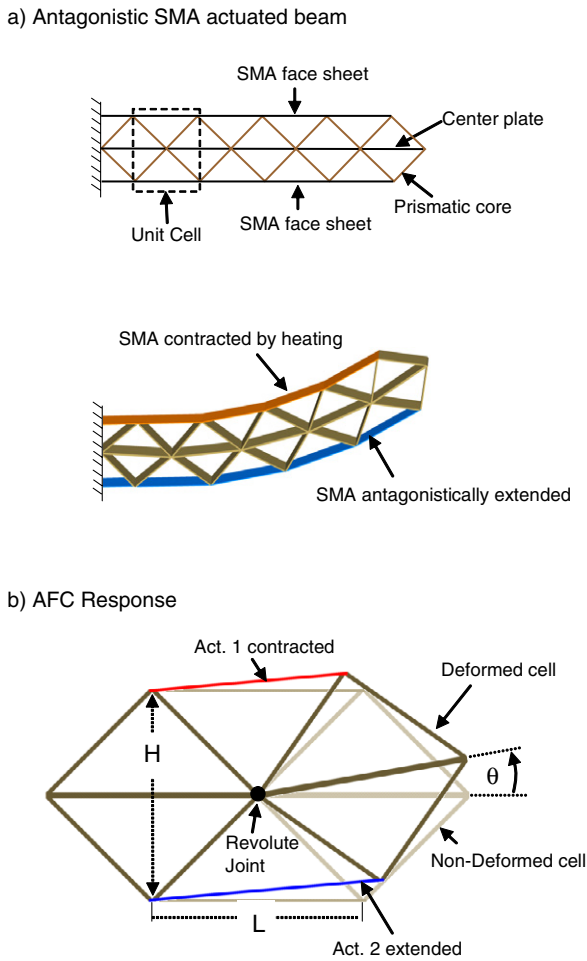


Figure 1. (a) Reversible SMA actuated beams created by linking antagonistic flexural unit cells (AFC). Heating one or other of the SMA facesheets causes a flexural deformation of the beam. (b) Unit cell analysis showing that the contraction of actuator 1 by heating rotates the cell about a revolute joint by an angle θ . This also causes the extension of actuator 2.

The strain, ε , refers to the strain in actuator 1 measured with respect to the original length (prior to the pre-straining) of the actuator. Note that the strain in actuator 2 is related to the strain in actuator 1 [11]:

$$\text{Strain in actuator 2} = (\varepsilon_1^s + \varepsilon_2^s) - \varepsilon. \quad (2)$$

If only one of the actuators, say actuator 1, is pre-strained, then the strain in actuator 2 simply becomes

$$\text{Strain in actuator 2} = \varepsilon_1^s - \varepsilon. \quad (3)$$

Shape memory actuated devices may be required to perform many cycles [12]. The actuator must therefore be capable of repeatedly undergoing a martensite de-twinning process (to accommodate pre-strain) followed by a martensite to austenite transformation. Furuya *et al*, however, observed that the stroke of a load-supporting SMA wire was dramatically diminished during repeated cycling (cooling/heating) [13, 14]. They also reported that the length of the wire gradually increased during repeated thermal cycling under load [13, 14].

Eggeler *et al* have observed a similar phenomenon in NiTi SMA springs but found that the degradation stabilized after about 100 cycles [15]. Friend [16] also observed similar effects in CuZnAl coil springs. There are also several reports of a rapid degradation of actuators based upon the two-way shape memory effect (TWSME) [17, 18].

The actuator displacement range (stroke) reduction and its residual cycling elongation [13–16] are believed to be related to the contribution of dislocation to the deformation incurred during each loading cycle. This contribution is a result of rearrangement of the dislocation distribution created during prior cycles and by dislocation multiplication during a new loading cycle [18]. Stabilization of the martensite variants that are most favorably inclined to the applied stress can also contribute to the degradation [14, 19]. This second mechanism is also the basis of the training process used in two-way shape memory actuators (the TWSME) [18]. The stroke reduction is reported to be independent of the residual elongation for the load-supporting wire and springs [13, 14].

Unlike the aforementioned actuators which use constant loads (a hanging weight) to create reversibility, the residual elongation of a SMA linear actuator can contribute to further stroke reduction for spring biased and antagonistic SMA actuating systems. For instance, if a 4% pre-strain was initially stored in an AFC actuator, and a 0.5% non-recoverable strain is accumulated in the actuators during its first cycle of actuation, the amount of available shape memory strain at the beginning of the second cycle is reduced to 3.5%, because the antagonistic approach requires that the total length of a pair of the actuators remain constant. This reduced shape memory strain results in the diminished shape recovery strain of the AFC cell because the recovery strain is directly related to the shape memory strain in the actuators [20]. It therefore results in a reduction in the flexural angle (θ) that can be achieved (see figure 2). The illustrated rotation ranges in the figure are for the inactive configurations (after cooling actuator 1 and 2 to ambient temperature).

The degradation in the deformation range of polycrystalline NiTi SMA depends on the grain size and texture [15, 16], the straining temperature [20], the prior thermomechanical history of the actuator material [18, 20, 21], the alloy's composition [20, 22] and load [23].

Here, we experimentally investigate the effect of degradation upon an antagonistic actuated structure constructed from near equi-atomic NiTi actuators [11]. We show that shape recovery is reduced by the repetitive actuation. However, the degradation is found to stabilize after a relatively small number of cycles. The effect of shape memory pre-strain on the degradation is then also investigated. Finally a thermomechanical treatment is suggested that reduces the degradation in the device response. The results can be used to determine the required pre-strains to achieve desired deformations of the antagonistic shape memory actuated structure.

2. Experimental methodology

In the experiment represented here NiTi ribbons with a Ni–50.6 at.% Ti composition were used. The austenite, martensite

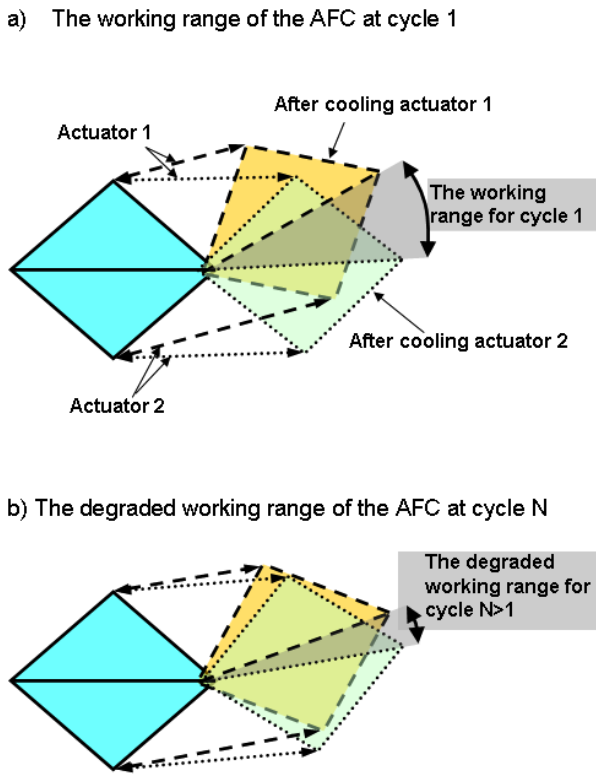


Figure 2. The rotation range (working range) is degraded during repeated loading.

and R-phase start and finish transformation temperatures were determined by differential scanning calorimetry (DSC) to be; $A_s = 56$, $A_f = 69$, $M_s = 23$, $M_f = -3$, $R_s = 51$ and $R_f = 43$ °C [11]. Therefore the samples are in R-phase after cooling from the austenite to ambient (25 °C). A linear antagonistic setup was used to study the repeated thermomechanical loading effect on the recovery strains of the actuators (figure 3) because it accurately simulates the equilibrium responses through a simple linear set up and without the need to build beam or

panel prototypes [11]. The NiTi samples were 0.25 mm thick and 7 mm wide. Each ribbon was 120 mm long with a 80 mm test span (20 mm of either side of each ribbon is held in the grips). Prior to pre-straining, both of the as-received ribbons were first heated in a tube furnace to 180 °C to remove stored deformations and subsequently cooled to room temperature (25 °C). One NiTi ribbon was then pre-strained to ϵ_1^s while the opposing element was left unstrained (figure 3(a)). The ribbons were then connected at one end by a mechanical fastener which electrically and thermally isolated them from each other and kept both actuators aligned. The other ends of the actuator pair were fixed to the grips of a tensile test instrument and a load cell used to measure the force exerted by the ribbons. The forces were then converted to stress by dividing by the original cross sectional area of the SMA ribbon.

During an experiment, pre-strained ribbon 1 was resistively heated above its austenite finish temperature, A_f (the actuators were heated to 110 °C in this experiment [11]), and then cooled to room temperature. The strain in ribbon 1 after its cooling is denoted ϵ_1^i (inactive equilibrium strain) [10]. During the second half of each actuation cycle, the opposite element (ribbon 2) was heated above the austenite finish temperature, A_f , and then cooled. This caused ribbon 1 to be extended compared to its length at the end of the first half of the cycle. The strain in ribbon 1 after heating and then cooling ribbon 2 is denoted by ϵ_2^i (both strains, ϵ_1^i and ϵ_2^i , refer to strain in ribbon 1). The strains in ribbon 1 during the heating-cooling of actuators 1 and then 2 were measured using a laser extensometer. The stress versus strain in actuator 1 is plotted in figure 4. The difference, $|\epsilon_1^i - \epsilon_2^i|$, is the inactive strain range [11]. By multiplying this strain range by the length of the ribbon, the deformation range of the actuator under ambient conditions can be determined.

The heating rate during the antagonistic cyclic experiment was controlled by the input power. The heating rate was selected to be relatively slow (1 °C s⁻¹) to accurately replicate the temperature history of the SMA ribbons in each cycle. The thermal cycle was then repeated by alternating heating

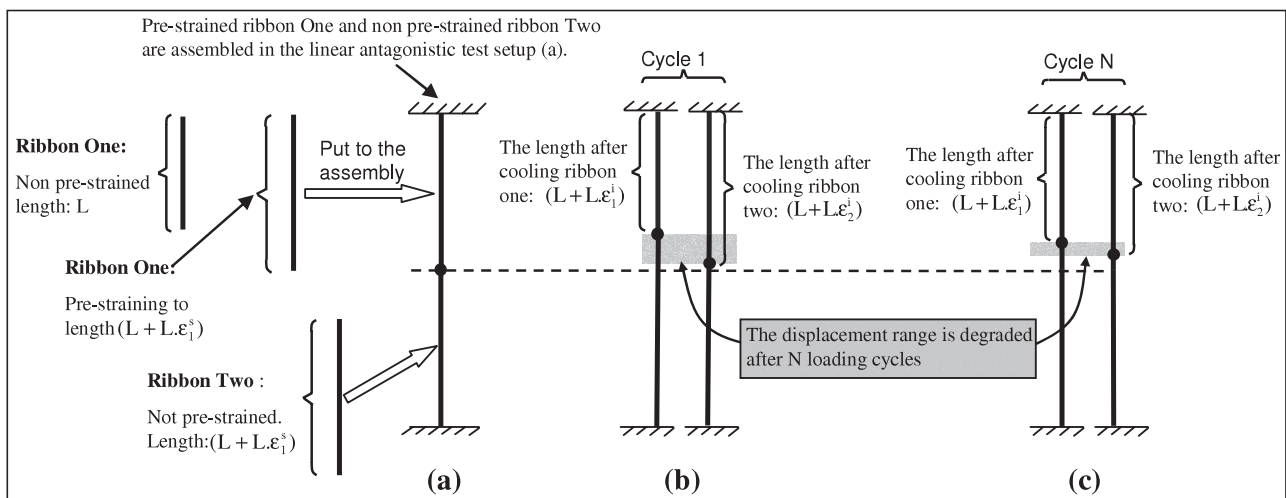


Figure 3. (a) The *in situ* antagonistic test setup [11]. (b) The inactive displacement range at the first cycle. (c) The displacement range is reduced after N cycles (degradation).

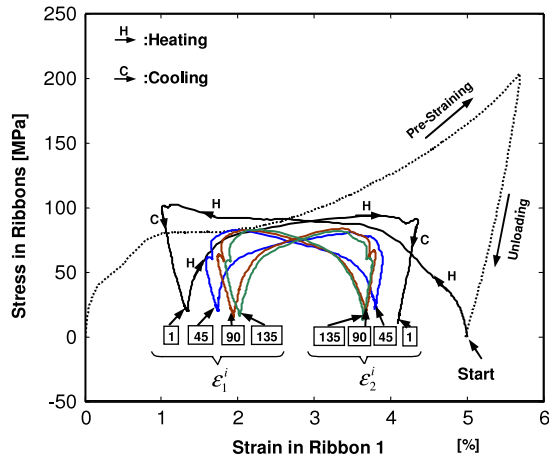


Figure 4. Cyclic stress–strain response for a 5% pre-strained antagonistic shape memory actuator. Cycles 14 590 and 135 are plotted for comparison. The superimposed dotted line is the 5% pre-straining process.

and cooling actuator 1 and then 2. The experiment was then repeated for several different pre-strains to study the relationship between degradation of the actuator and its pre-strain.

3. Results and discussion

3.1. Cyclic degradation

The flexural degradation of an AFC is illustrated in figure 2. The linear displacement degradation in a linear antagonistic setup equivalent to the AFC is also shown (figure 3). During cycling, the length of actuator 1 after cooling it to the ambient temperature after repeated loading (figure 3(c)) was always larger than that after the first cycle (figure 3(b)). As a result (after conversion of the displacement to strain), ϵ_1^i was increased as the actuator was thermomechanically cycled in the AFC device. Similarly, the final length of actuator 1 after cooling actuator 2 (figure 3(c)) was less than its length at the end of cycle 1 (figure 3(b)), indicating that ϵ_2^i was reduced by cycling. As a result, the actuator stroke at the ambient temperature (the shaded distance in figure 3) was degraded. Degradation of the antagonistic actuators can therefore be defined as the reduction of $|\epsilon_2^i - \epsilon_1^i|$ during repeated loading.

The stress versus strain (in actuator 1) resulted from an antagonistic experiment with a 5% pre-strained setup is plotted in figure 4. A detailed analysis of the first cycle is presented elsewhere [11]. The stress–strain curves for cycles 45, 90 and 135 are plotted together with the first cycle figure 4. From the figure it is apparent that the strain range degradation has slowed down at about 100 cycles.

Figures 4 and 5 illustrate that the rate of reduction of the strain range, $|\frac{d(\epsilon_1^i - \epsilon_2^i)}{dN}|$, decreases during cycling loading. Figure 5 also shows that after about 100 complete cycles this rate vanishes and the strain range is then stabilized (figure 5). Therefore in this research cycle 100 was chosen to be the cutting-off cycle for all the data points for comparison. This is consistent with the work done by Gall and Maier [19]

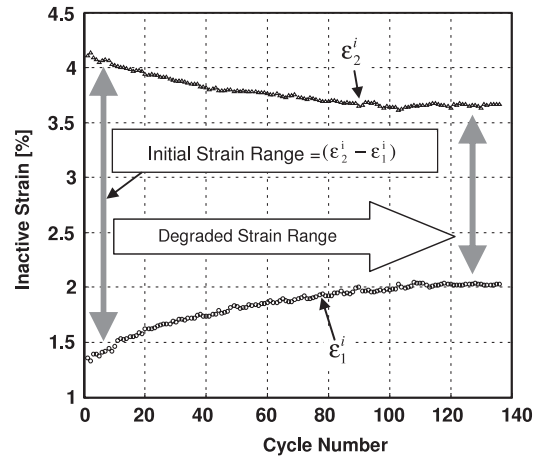


Figure 5. The recovered strains (inactive strain) of a 5% pre-strained antagonistic shape memory actuator are stabilized after about 100 cycles (the degradation ceases).

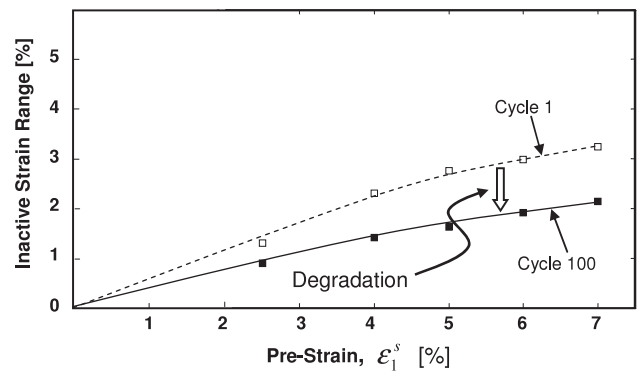


Figure 6. The degradation of an SMA antagonistic actuator depends upon pre-strain.

who investigated the mechanical cycling and degradation of samples made of NiTi single crystals. However, to investigate the effect of high cycle degradation, the test can be continued.

3.2. Pre-strain effects

The effect of pre-strain on the degradation was studied by preparing separate 2.5, 4, 6 and 7% pre-strained samples and testing them in the same manner as the 5% pre-strained actuator. Recall that in the 5% pre-strained actuator, the strain range stabilized at about 100 cycles. Figure 6 summarizes the effect of pre-strain on the inactive strain degradation of the antagonistic NiTi actuated linear test device. The magnitude of the degradation of the actuators after 100 cycles is indicated by a downward arrow in figure 6. It can be seen that the final working range of the antagonistic actuator increases with pre-strain.

Clearly, if a large stabilized recoverable strain is required then a high actuator pre-strain must be used. However, it is important to recognize that increasing the pre-strain also increases the recovery force. The antagonistic shape memory device must therefore withstand larger forces for the first few cycles until the degradation stabilizes. The maximum value of

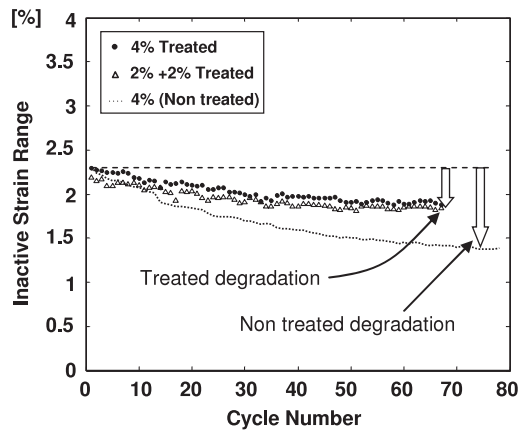


Figure 7. The effect of thermomechanical treatment on the degradation of 4% pre-strained antagonistic actuators. Such treatments can be used to significantly reduce the degradation of antagonistic shape memory actuated devices.

the force can be found from the cyclic test result. For instance, figure 4 shows for an antagonistic setup with 5% pre-strain that the maximum stress is generated at the end of the first heating in the first cycle. It corresponds to a stress of 103 MPa. The same method can be used to find the maximum stress for the other pre-strains.

3.3. Thermomechanical treatment

Simple thermomechanical treatment has been discovered to reduce degradation of AFC actuated structures. The NiTi ribbons are cycled in the antagonistic test setup (figure 3) to stabilize the favored martensite variants. The cycled NiTi ribbons are removed from the test rig and pre-strained and then assembled in the test setup to observe the evolution of the degradation.

An example experiment used a ribbon that was pre-strained to 6% and then assembled in the linear antagonistic setup (figure 3) with another ribbon. The set up was then cycled 150 times until the stabilization of the deformations. Both ribbons were then removed and heated to 180 °C to remove the stored deformations. After this treatment, one ribbon (say ribbon 1) was pre-strained to 4% and the antagonistic setup was reassembled. The inactive strain range is plotted in figure 7 and is referred in the figure as '4% treated'. In another test, two separate ribbons were subjected to the same thermomechanical treatment. This time both ribbons were pre-strained to 2% before reassembly of the antagonistic test set up. The total shape memory strain is therefore 4% (2% each ribbon) for comparison with the '4% treated'. The strain range versus cycle number for the second treatment (called '2%+2% treated') is marked in figure 6 by empty circles. The strain versus cycle number of a 4% non-treated antagonistic actuator (no cyclic treatment is performed on the ribbons before the assembly) is also plotted in the figure for comparison (plotted as the dotted line and marked as '4% non-treated'). The degradation is still observed in the three cases; however, it is apparent in figure 7 that the degradation is significantly less severe in the treated samples. In addition, the strain range

of the treated actuators somewhat flattens at about cycle 50 as compared to the 100 cycles for the non-treated actuators (figure 5). Although the general trend for the degradation of the '4% treated' and the '2%+2% treated' are similar (compare the filled circles with hollow triangles in figure 7), the 4% treated one shows a larger working range.

4. Conclusion

The stroke of the antagonistic SMA actuators significantly decreases during cycling (degradation). The degradation is shown to cease after about 100 cycles of operation. While the actuator stroke degradation is increased with SMA pre-strain the stabilized strain is still increased with pre-strain. A simple thermomechanical treatment was shown to reduce the degradation of antagonistic NiTi actuators.

References

- [1] Otsuka K and Wayman C M 1998 *Shape Memory Materials* (New York: Cambridge University Press)
- [2] Benard W L, Kahn H, Heuer A H and Huff M A 1998 Thin-film shape-memory alloy actuated micropumps *J. Microelectromech. Syst.* **7** 245–51
- [3] Hunter I W, Lafontaine S, Nielsen P M F, Hunter P J and Hollerbach J M 1990 Manipulation and dynamic mechanical testing of microscopic objects using a tele-micro-robot system *IEEE Control Syst. Mag.* **10** 3–9
- [4] Johnson A D, Gupta V, Martynov V and Menchaca L 2003 Silicon oxide diaphragm valves and pumps with TiNi thin film actuation *Proc. Int. Conf. on Shape Memory and Superelastic Technologies (Pacific Grove, CA)* pp 605–12
- [5] Hinkley D and Simburger E J 2001 A multifunctional flexure hinge for deploying Omnidirectional solar arrays *Proc. 42nd AIAA/ASME/ASCE/AHS/ASC Structures, Structural Dynamics and Materials Conf. (Seattle, Washington, AIAA)* p 1260
- [6] Duerig T W, Melton K N, Stöckel D and Wayman C M 1990 *Engineering Aspects of Shape Memory Alloys* (UK: Butterworth-Heinemann)
- [7] Elzey D M, Sofla A Y N and Wadley H N G 2002 Shape memory-based structural actuator panel *Proc. SPIE* **4698** 192–200
- [8] Elzey D M, Sofla A Y N and Wadley H N G 2005 A shape memory-based multifunctional structural actuator panel *Int. J. Solids Struct.* **42** 1943–55
- [9] Elzey D M, Sofla A Y N and Wadley H N G 2003 A bio-inspired, high authority actuator for shape morphing structures *Proc. SPIE: Smart Structures and Materials: Active Materials Behavior and Mechanics* **5053** 92–100
- [10] Sofla A Y N, Elzey D M and Wadley H N G 2004 An antagonistic flexural unit cell for design of shape morphing structures *Proc. IMECE2004 (Anaheim, CA: ASME)*
- [11] Sofla A Y N, Elzey D M and Wadley H N G 2008 Two-way antagonistic shape actuation based on the one-way shape memory effect *J. Intell. Mater. Syst. Struct.* at press (published online Dec. 2007)
- [12] Hornbogen E 2004 Thermo-mechanical fatigue of shape memory alloys *J. Mater. Sci.* **39** 385–99
- [13] Furuya Y, Shimada H, Matsumoto M and Honma T 1988 Cyclic deformation and degradation in shape memory effect of Ti–Ni wire *J. Japan Inst. Met.* **52** 139–43
- [14] Furuya Y, Shimada H, Matsumoto M and Honma T 1989 Fatigue and degradation of shape memory effect in Ti–Ni wire *MRS Intl. Mtg. Adv. Mets.* vol 9, pp 269–74

- [15] Eggeler G, Hornbogen E, Yawny A, Heckmann A and Wagner M 2004 Structural and functional fatigue of shape memory alloys *Mater. Sci. Eng. A* **378** 24–33
- [16] Friend C M 1987 Shape-strain degradation in CuZnAl coil-spring reversible shape-memory actuators *Scr. Metall.* **12** 581–5
- [17] Edo S 1989 Shape deterioration and reversible shape-memory effect in Ni–Ti alloys *J. Mater. Sci.* **24** 3991–3
- [18] Scherngell H and Kneissl A C 1998 Training and stability of the intrinsic two-way shape memory effect in Ni–Ti alloys *Scr. Mater.* **30** 205–12
- [19] Gall K and Maier H J 2002 Cyclic deformation mechanisms in precipitated NiTi shape memory alloys *Acta Mater.* **50** 4643–57
- [20] Miyazaki S, Imai T, Igo Y and Otsuka K 1986 Effect of cyclic deformation on the pseudoelasticity characteristics of Ti–Ni alloys *Metall. Trans. A* **17A** 115–20
- [21] Strnadel B, Ohashi S, Ohtsuka H, Ishihara T and Miyazaki S 1995 Cyclic stress–strain characteristics of Ti–Ni–Cu shape memory alloys *Mater. Sci. Eng. A* **202** 148–56
- [22] Strandel B, Ohashi S, Ohtsuka H, Miyazaki S and Ishihara T 1995 Effect of mechanical cycling on the Pseudoelasticity of Ti–Ni and Ti–Ni–Cu alloys *Mater. Sci. Eng. A* **203** 187–96
- [23] Van Humbeek J 1990 Shape memory alloys: the phenomenon, the materials, their properties and applications *Trait. Therm.* (234) 20